Pure appl. geophys. 165 (2008) 2229–2248
0033–4553/08/112229–20
DOI 10.1007/s00024-008-0424-7

Pure and Applied Geophysics

An Efficient and Robust Tsunami Model on Unstructured Grids. Part I: Inundation Benchmarks

YINGLONG J. ZHANG[1] and ANTÓNIO M. BAPTISTA[1]

Abstract—A modern multi-purpose baroclinic circulation model (SELFE) has been recently extended to include the ability to simulate tsunami propagation and inundation. The core model is based on the 3-D nonlinear shallow-water wave (NSW) equations, which are solved on unstructured grids, using the finite-element method. A semi-implicit method is used to solve all equations to enhance numerical stability, thus bypassing the most stringent CFL restriction on the time step. Further aided algorithmically by an Eulerian-Lagrangian solution of the advection terms in the momentum equation and by a simple yet effective inundation algorithm, SELFE is very efficient and robust in both quasi-2-D (with two vertical layers) and 3-D modes. A quasi-2-D version of the model is being used to update and expand the characterization of tsunami hazards along the Oregon coast. As a part of a rigorous testing procedure that includes multiple types of coastal problems, we present in this paper a quantitative assessment of performance of the quasi-2-D SELFE for two challenging open benchmark problems proposed in the 3rd International Workshop on Long-wave Runup Models. Satisfactory results are obtained for both problems.

Key words: Tsunami inundation, cross-scale modeling, finite elements, semi-implicit model, Eulerian-Lagrangian Method.

1. Introduction

The Indian Ocean mega-tsunami of 2004 dramatically reinforced the importance of tsunami hazard assessment and mitigation, and challenged all involved communities to re-evaluate their strategies for a holistic analysis of risk.

In the United States, the State of Oregon has been pro-active in tsunami hazard assessment and mitigation since the early 1990s, when, in the wake of the Nicaragua and Okushiri tsunamis of 1992 and 1993, and prompted by newly found evidence of a tsunamogenic Cascadia Subduction Zone, the Oregon Department of Geology and Mineral Industries (DOGAMI) developed a state-wide tsunami hazard map (PRIEST, 1995). That work has been refined over the years through a series of local studies, leading progressively to highly detailed community-specific inundation maps that help coastal

[1] Science and Technology Center for Coastal Margin Observation and Prediction, Oregon Health & Science University, 20000 NW Walker Road, Beaverton, OR 97006, U.S.A. E-mail: yinglong@stccmop.org

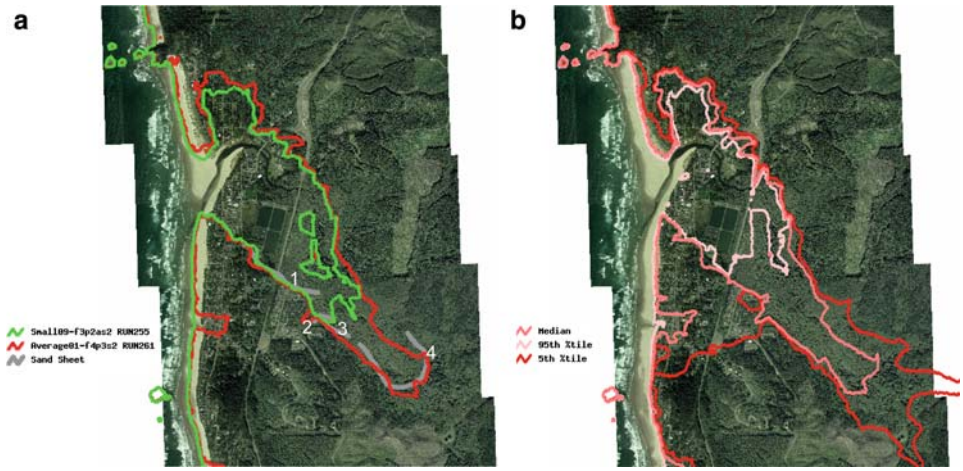

Figure 1
(a) Paleo-tsunamis on Cannon Beach, Oregon. The four sand sheets were collected by Dr. Rob Witter of DOGAMI and indicate the minimum extent of inundation due to past tsunami events. Sheets 1 and 2 are attributed to small events, and sheets 3 and 4 to average to large events. Also shown are the maximum inundation extent calculated using the model for typically small and average tsunami events on inferred paleo-landscapes around Cannon Beach. (b) Quasi-probabilistic inundation map for Cannon Beach, based on the results for 25 scenarios (8 cases each for average, large and largest events, plus 1 case for small events).

planners increase community preparedness, in part through education and raised awareness supported by evacuation maps and well-marked evacuation routes. Also, bridges have been upgraded based on perceived risk, and new critical infrastructure (such as hospitals and schools) has been located so as to minimize risk.

Recent tsunami studies in Oregon have been conducted with a multi-disciplinary approach that (a) attempts to characterize the underwater earthquake source based on best-available geological and seismic evidence, including but not limited to analyses of turbidite data (Goldfinger *et al*., 2003) and sand tsunami deposits contained in cored samples (Witter *et al*., 2003; Fig. 1a); and (b) embraces a probabilistic concept of risk (Fig. 1b). A similar multi-disciplinary approach towards the probabilistic tsunami hazard analysis was also conducted at Seaside, Oregon by the Tsunami Pilot Study Working Group (2006). The combination of (a) and (b) entails hundreds of tsunami simulations, which could not be realistically accomplished by the numerical hydrodynamic model (ADCIRC; Luettich *et al*., 1991) that we have used over the past ten years to study the propagation and coastal inundation of Cascadia Subduction Zone (CSZ) tsunamis.

This led us to evaluate the potential of two very efficient 3-D circulation models (ELCIRC, Zhang *et al*., 2004; and SELFE, Zhang and Baptista, 2008), developed in recent years to sustain advanced modeling within ocean observatories (Baptista, 2006), as reference models for our tsunami studies. This is the first of a series of papers that report on the extension of these models to tsunami simulations. Our focus in this article is on inundation modeling, and in particular on benchmarking one of the models (SELFE)

against analytical and laboratory tests. We will report elsewhere on the results of the validation of the models against field data in the well documented 1993 Hokkaido-Nansei-Oki tsunami (Myers and Baptista, 1995; Shimamato *et al*., 1995), and on applications to Cascadia Subduction Zone tsunamis. As general cross-scale ocean models, SELFE and ELCIRC have also been cross-applied to a range of coastal margin processes, including characterization of 3-D estuarine and plume circulation, in which context they have been extensively validated against field data (Baptista *et al*., 2005; Zhang and Baptista, 2008).

The paper is organized as follows. After this introduction, we place the development of SELFE in context of the state-of-the-art in hydrodynamic modeling of tsunamis (Section 2). We then summarize the main SELFE physical and numerical formulations, including the new inundation algorithm (Section 3). Results from benchmarking SELFE with two challenging initial- and boundary-value problems are presented in Section 4. Conclusions and road maps for future work are presented in Section 5.

2. *SELFE in Context of the State-of-the-Art of Tsunami Modeling*

Over the past two decades tremendous progress has been made in numerical modeling of tsunamis, from its generation (source model) to propagation through the open ocean to final inundation on dry land (propagation and inundation model). Uncertainties exist in all stages of simulation, with arguably the largest occurring in the initial stage: The characterization of the earthquake/landslide source of the tsunami (Wang and He, 1999; Synolakis and Bernard, 2006). However, reducing errors in the propagation and inundation of the tsunami wave remains an important challenge, not only because of the need to improve the characterization/comparison of impacts for defined sources, but also to improve the ability to characterize sources post-event via inversion of sea-level data (arguably not a well posed problem without better propagation/inundation models; see Synolakis and Bernard, 2006; Wei *et al*., 2008).

Increasingly sophisticated methods have been proposed to tackle the high nonlinearity and supercritical flow as found in the propagation and, in particular, inundation processes. These models usually solve shallow-water wave equations (either linear (LSW) or nonlinear (NSW), in which the wave dispersion is neglected), or Boussinesq or Euler equations which incorporate dispersion effects, in 1-D, 2-D or 3-D. Smoothed Particle Hydrodynamics (SPH) also showed promise recently (Dias and Dutykh, 2007). Most popular models of the current generation are so-called "2 + 1" models (i.e., depth-averaged in space plus time evolution) based on the NSW equations. Among others, Titov and Synolakis (1995) demonstrated that except in the wave-breaking region, the NSW formulation was able to accurately predict long wave runup. On the other hand, the NSW formulation may not be appropriate for dispersive waves as found in trans-oceanic and in many landslide-generated tsunamis (Liu *et al*., 2005), for which a Boussinesq or Euler formulation may be necessary. Burwell *et al*. (2007) presented an approach to use numerical dispersion to mimic physical dispersion.

With few exceptions, most current numerical tsunami models use the finite-difference method on structured rectangular grids (Titov and Synolakis, 1995; Lynett *et al*., 2002; Yalciner *et al*., 2002). A recent notable exception to finite differences was introduced by George and LeVeque (2006) and LeVeque and George (2007), who used a Godunov-type finite-volume method for enforcing conservation properties and obtained excellent results for some benchmark problems. In addition, they also proposed an adaptive mesh refinement strategy. However, the flux limiter used is one-dimensional in nature and its extension to the transverse direction is still problematic.

More than the use of finite differences, the general preference for structured grids is somewhat surprising. Indeed, the complex geometry and bathymetry/topography of coastlines are often responsible for many intriguing localized inundation patterns (e.g., the large runup in a narrow valley in the Okushiri Island in the 1993 Hokkaido-Nansei-Oki tsunami, see Shimamato *et al*. (1995); Nicaragua tsunami, see Baptista *et al*., 1993). The natural ability of structured grids to accurately resolve these important features is limited, and therefore various grid nesting or adapting approaches have been proposed to address localized refinement (Venturato *et al*., 2007; George and LeVeque, 2006). The proper imposition of boundary conditions at the interfaces between grids of various resolutions remains a challenging issue (Venturato *et al*., 2007).

By contrast, unstructured grids have the inherent ability to resolve complex geometry and bathymetry/topography. Yet, relatively few such models have been used on a sustained basis for practical tsunami propagation and inundation studies. An exception is ADCIRC (Luettich *et al*., 1991), a model that we adapted to tsunamis in the mid-1990s (Myers and Baptista, 1995, 1997, 2001; Myers, 1998; Myers *et al*., 1999). Originally written as a general circulation model, and based on the solution of the Generalized Wave-continuity equation (GWCE; Lynch and Werner, 1991) by finite elements on unstructured grids, ADCIRC has — in an interesting contrast between closely related fields — been extensively used in inundation studies for storm surges and hurricanes (Westerink *et al*., 2004).

Our experiences with ADCIRC as a tsunami propagation and inundation model were mixed. While the model was transformative in extensively mapping tsunami inundation in the Oregon coast (Priest, 1995; Priest *et al*., 1995, 1997a, 1997b, 1998, 1999a, 1999b, 2000, 2002, 2003; Priest and Baptista 2000), some numerical limitations became apparent. Issues related to volume/mass conservation and to parasitic oscillations, due to the use of GWCE in lieu of the primitive momentum equations,[1] were particularly of concern. Also, numerical stability constraints forced very small time steps to be used, resulting in computational inefficiency. Finally, the inundation algorithm could lead to serious instabilities during the inundation in benchmark problems as described in the review paper by Synolakis and Bernard (2006).

[1] Recently there has been some progress in incorporating the Discontinuous Galerkin Finite-Element method in ADCIRC in order to use the primitive equations; see Kubatko *et al*. (2006). However, the efficiency problem remains an issue.

The recent development of a new generation of very efficient 3-D unstructured grid circulation models (such as UnTRIM, Casulli and Walters, 2000; ELCIRC, Zhang *et al*., 2004; SELFE, Zhang and Baptista, 2008; and FVCOM, Chen *et al*., 2003), whose performance in realistic simulations of estuarine and coastal dynamics rivals or surpasses ADCIRC, has created the opportunity to revisit options available for unstructured grid modeling of tsunamis. The main goal of the present work is to introduce a tsunami propagation and inundation version of SELFE. Based on the finite-element solution of the primitive NSW equations, SELFE is hydrostatic, and hence is not currently suited for problems in which wave dispersion effects are important. Yet, the physics of SELFE is essentially the same as in MOST, a reference model used by NOAA in tsunami simulations worldwide and originally developed by Titov and Synolakis (1995).

SELFE uses semi-implicit time stepping and treats the advection with an Eulerian-Lagrangian method (ELM; Baptista, 1987), and therefore most stringent stability conditions (e.g., CFL) are bypassed, resulting in greater efficiency. The matrices in the model are all positive definite and symmetric, and very efficient solvers like the Conjugate Gradient (CG) method can be used with fast convergence guaranteed. The well-conditioning of the matrices and a simple yet effective inundation algorithm lead to great robustness of the model; only minimal instabilities are encountered near the wetting and drying interface, even without bottom friction and viscosity. Compared to ADCIRC, the new model is considerably more efficient, conserves volume and mass well, and suffers little from the parasitic oscillations. Therefore the model is well suited for realistic applications, including forecasting.

Since the original model was 3-D, and incorporates baroclinicity as well as realistic tidal and atmospheric forcings, the new tsunami model can simulate these effects in a straightforward fashion.[2] The importance of nonlinear interactions between tides and tsunami waves has been demonstrated in Myers (1998). Three-dimensional effects are also important in landslide-generated tsunamis (Liu *et al*., 2005). However, better physical formulations (e.g., dispersion effects, small-scale turbulence etc.) may be needed in order to take full advantage of the 3-D model. These formulations will be considered in the future model.

3. *Physical and Numerical Formulation of SELFE*

The equations SELFE solves are the 3-D nonlinear shallow-water wave (NSW) equations, transport equations for salt and heat, and turbulence closure. Since only the barotropic model is used in this paper, the transport and turbulence closure equations are not included in this paper; however, we note that these are existing capabilities of the model. The equations used in the tsunami model are then:

[2] 3D tsunami simulations are inevitably expensive, but with the judicious use of unstructured grid and a parallel code that became available recently, the current model is able to do such simulations.

$$\nabla \cdot \mathbf{u} + \frac{\partial w}{\partial z} = 0 \tag{1}$$

$$\frac{\partial(\eta - b)}{\partial t} + \nabla \cdot \int_{-h}^{\eta} \mathbf{u} dz = 0 \tag{2}$$

$$\frac{D\mathbf{u}}{Dt} = \mathbf{f} - g\nabla\eta + \frac{\partial}{\partial z}\left(\nu \frac{\partial \mathbf{u}}{\partial z}\right);$$

$$\mathbf{f} = -f\mathbf{k} \times \mathbf{u} + \alpha g \nabla\hat{\psi} - \frac{1}{\rho_0}\nabla p_A - \frac{g}{\rho_0}\int_{z}^{\eta} \nabla\rho \, d\zeta + \nabla \cdot (\mu \nabla \mathbf{u}) \tag{3}$$

where

(x,y)	horizontal Cartesian coordinates, in $[m]$
z	vertical coordinate, positive upward, in $[m]$
∇	$\left(\frac{\partial}{\partial x}, \frac{\partial}{\partial y}\right)$
t	time $[s]$
$\eta(x, y, t)$	free-surface elevation, in $[m]$
$b(x,y,t)$	seabed displacement in $[m]$ (positive for uplift)
$h(x, y)$	bathymetric depth, in $[m]$
$\mathbf{u}(x, y, z, t)$	horizontal velocity, with Cartesian components (u,v), in $[ms^{-1}]$
w	vertical velocity, in $[ms^{-1}]$
f	Coriolis factor, in $[s^{-1}]$
g	acceleration of gravity, in $[ms^{-2}]$
$\hat{\psi}(\phi, \lambda)$	earth-tidal potential, in $[m]$
α	effective earth-elasticity factor
$\rho(\mathbf{x}, t)$	water density; by default, reference value ρ_0 is set as 1025 kgm^{-3}
$p_A(x, y, t)$	atmospheric pressure at the free surface, in $[Nm^{-2}]$
ν	vertical eddy viscosity, in $[m^2\ s^{-1}]$
μ	horizontal eddy viscosity, in $[m^2\ s^{-1}]$

Comparing these equation to those in Zhang and Baptista (2008), the only difference is in Equation (2), where the bed deformation is included, and therefore the current model is capable of simulating the initial seabed movement during the earthquake. This is important because in real tsunamis the initial acceleration is very large despite the initial velocities being small, and therefore strictly speaking, an elevation field that mirrors the bed deformation with zero velocity everywhere is not the right initial condition (Dutykh *et al.*, 2006; Kanoglu and Synolakis, 2006). All equations have appropriate initial and boundary conditions.

Since a detailed description of the numerical formulation is given in Zhang and Baptista (2008), only a brief summary is given here. The horizontal domain is discretized into a series

of triangular elements (unstructured grid technique), and the vertical dimension is divided into layers. A semi-implicit finite-element method is used to solve the coupled continuity and momentum Equations (2) and (3); a key step is to decouple the two equations through the bottom boundary layer. The advection in Equation (3) is treated with ELM, which is explicit but unconditionally stable (Baptista, 1987). A finite-volume method is used to solve the continuity Equation (1). The resulting matrices are all symmetric and positive-definite if a mild restriction is placed on the water depth (Zhang and Baptista, 2008), and therefore the numerical scheme is very efficient and robust. If the horizontal viscosity is not used, there is no stability constraint in the current model and large time steps could be used; however, a smaller time step is necessary to ensure accuracy because of the relatively short period for tsunami waves (Walters, 2005) and the highly nonlinear inundation process.

As regards the tsunami simulation, we found that one of the most critically important issues is related to the inundation algorithm. The wetting and drying process can be treated in a relatively straightforward fashion based on the water depths in SELFE (Zhang and Baptista, 2008). The challenges of the inundation algorithm and the solution thereof will be detailed in the following subsection.

3.1. Inundation Algorithm

The inundation process as found in typical tsunamis is a highly complex and nonlinear moving-boundary problem, and some processes such as overland flow, scoured sediments and wave breaking have not been fully understood. However, for practical estimates of inundation extent and maximum wave runups, Titov and Synolakis (1995) showed that NSW formalism gives remarkably good results. From a numerical viewpoint, while a moving/adaptive grid is conceptually more efficient in capturing the moving shoreline (e.g., Hubbard and Dodd (2002) proposed a hierarchical Cartesian Adaptive Mesh Refinement (AMR) algorithm that largely bypassed the need for tracking the shoreline), it does pose some robustness issues as the flow is supercritical near the wetting and drying interface (Venturato *et al*., 2007). Therefore we use fixed meshes, and in doing so preclude partial wetting and drying in an element. This drawback is remedied by using high resolution near the wetting and drying interfaces, which is made possible by judicious use of an unstructured grid.

The inundation algorithm used in SELFE is intuitive and relatively straightforward. At the beginning of each time step, the interfaces (or shorelines) between wet and dry regions are computed. Then at the end of that time step, each node on the interfaces is examined in turn to determine if the interface there needs to be advanced or retreated. The interfaces are then updated and the process is repeated until new interfaces are found. The procedure is summarized as follows:

1. Compute wet/dry interfaces (Γ^n) at time step n (Fig. 2a);
2. At the end of time step $n + 1$, go through and examine all interfacial nodes on Γ^n. If a node (say, A) is surrounded by wet elements (with all nodes being wet-based on

newly computed elevations), the local interface line is advanced into the dry region, and the velocity at the center of the dry side is calculated as the average of the adjacent sides (Fig. 2b). If one or more elements surrounding a node (say, B) are dry (based on newly computed elevations), the local interface line is retreated towards the wet region;

3. Update interface lines based on the results from step 2, and iterate until the final interface lines at the step $n + 1$ (Γ^{n+1}) are found (Fig. 2c);
4. Go through all nodes on Γ^{n+1}, and do constant extrapolation of the elevations into the dry region (e.g., elevation(A'') = elevation(A')) if the total volume flux from the adjacent sides on the interface is into the dry region (Fig. 2d).

Note that step 4 is similar to the extrapolation procedure in TITOV and SYNOLAKIS (1995), and is an effective way to smooth numerical instabilities commonly found near the interfaces; otherwise the large elevation gradients near the interfaces would lead to unrealistically large velocity.

4. Benchmarks

As expounded in SYNOLAKIS and BERNARD (2006) and SYNOLAKIS *et al.* (2007), inundation models need to be carefully benchmarked against three types of data: analytical solutions, laboratory data, and field measurements. Due to the enormous uncertainties in most real-case tsunamis, the comparisons with known analytical solutions and laboratory data are critically important to gain confidence in the numerical model. Therefore in this paper, we present the results for the first two benchmark tests published by the 3rd International Workshop on Long-wave Runup Models (IWLRM, LIU *et al.*, 2008; http://www.cee.cornell.edu/longwave/index.cfm?page=benchmark&problem=1). The evaluation of model performance in real tsunami applications (1993 Hokkaido-Nansei-Oki, 1964 Alaska, and historical tsunamis caused by Cascadia Subduction Zone earthquakes, etc.) is left to future publications.

4.1. Wave Runup on a Uniform Plane Beach

The first problem has a simple setup, with a uniformly sloping beach and no variation in the lateral direction, and therefore is a 2-D problem in the vertical plane. The only forcing is the initial displacement of the free surface that resembles a typical *N*-wave, with a leading-depression wave followed by an elevation wave, as found in most tsunamis (Fig. 3). The initial-value-problem (IVP) technique introduced by CARRIER *et al.* (2003), and later improved by KÂNOGLU (2004), provides a nonlinear analytical solution, which can be downloaded from the IWLRM website. IVPs are particularly challenging for numerical models as the inherent numerical dissipation in a model will become quite apparent due to the lack of continuous supply of energy into the domain as found in

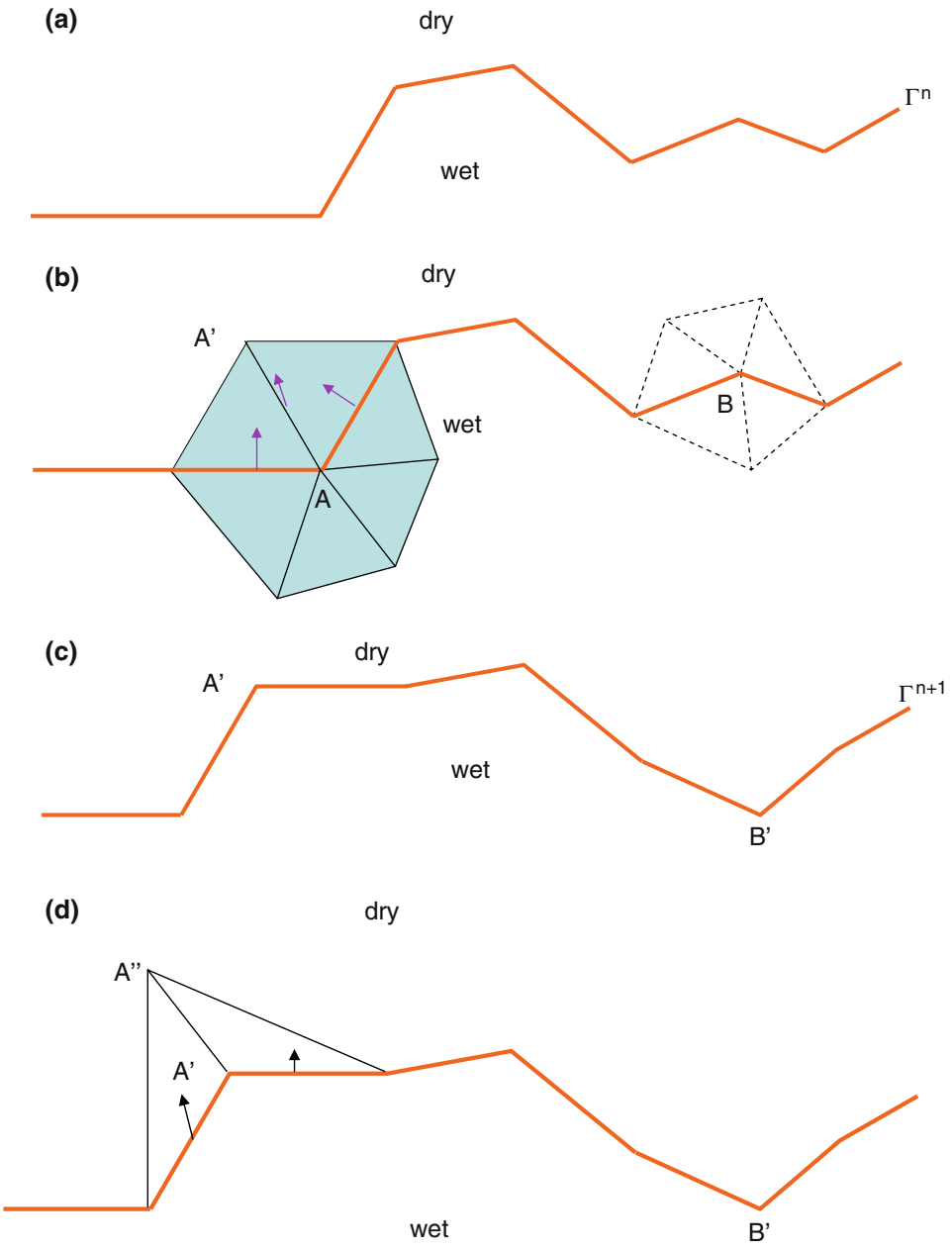

Figure 2
The inundation algorithm in SELFE. (a) Initial wet/dry interface at step n; (b) evaluate wet/dry status for interfacial nodes based on new elevations at step $n + 1$; (c) update the wet/dry interface, and iterate between (b) and (c); (d) final extrapolation of elevations along the final interface.

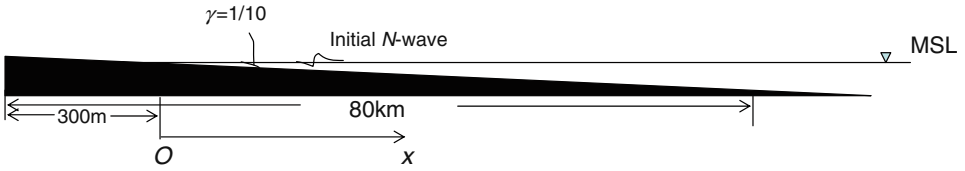

Figure 3
Definition sketch of the plane beach runup test. Depth in the domain is $x/10$.

boundary-value problems; in other words, the energy loss due to excessive numerical dissipation would lead to poor results in IVPs.

The initial shoreline is at $x = 0$ (Fig. 3), and the domain is about 80 km long, with the region between $x = -300$ m to $x = 0$ being initially dry. The large domain was chosen to minimize the reflection from the right boundary, where a radiation boundary condition was imposed. Various grid resolutions, ranging from 40 m to 2.5 m, were tested, but only uniform grids (by splitting each rectangle into 2 triangles) were used for simplicity and to facilitate the convergence study (see below). In other words, we did not take full advantage of using an efficient variable-resolution unstructured grid in this study. Two vertical layers were used in the vertical direction, and therefore essentially a 2-D depth-averaged model was used. The time step was fixed at 0.1 s. Although a much larger time step can be used without comprising numerical stability, a small time step was chosen for accurate simulation of the inundation process.[3] The implicitness factor was set to be 1 (i.e., fully implicit). Bottom friction and viscosity were all neglected in order to be consistent with the analytical solution. The run was carried out for a total of 600 sec, but most comparisons were done for the first 300 sec. All runs shown in this paper were carried out on an AMD Opteron 2.2 GHz processor. With $\Delta x = \Delta y = 5$ m and a grid with 176011 nodes, the 600 sec-run took 16 hours CPU time.

The initial amplitude of the *N*-wave is about 12 m, which translates to a very large extent of inundation (over 36 m in the vertical and 400 m in the horizontal excursion of the shoreline; Fig. 4), and supercritical flow near the shoreline (Fig. 5). The comparison of instantaneous surface elevations and velocity in the x direction at three time instances ($t = 160$, 175, and 220 sec) is presented in Figure 4. The 2nd and 3rd time instances roughly correspond to maximum drawdown and runup. The model results for elevation are excellent for all stages of the wave, with an error of 4.7% for the predicted maximum runup, which is within the error limit proposed in Synolakis *et al*. (2007). Larger errors in the velocity are observed, especially near the shoreline; probably due to numerical dissipation, the model seems to have lost some energy in that region.

The comparison of shoreline position and velocity is shown in Figure 5. The average and maximum errors in the predicted shoreline position are 10 m and 40 m, respectively.

[3] For real applications, a variable time step approach is usually used; the model is run with a larger time step (e.g., 5–10 s) until the first wave hits the coastline and then the time step is reduced to capture the inundation.

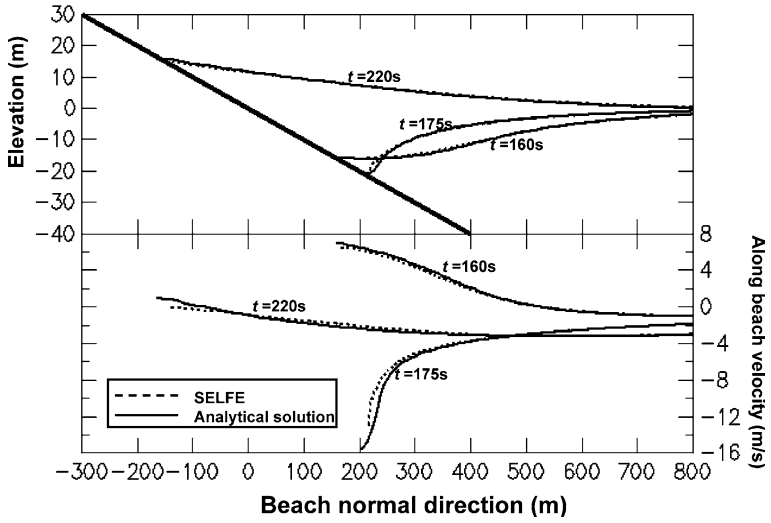

Figure 4
Comparison of instantaneous free surface (top panel) and velocity (bottom panel) along the plane beach at three time instances. The thick black line in the top panel indicates the bottom position.

Again, larger errors are observed in the shoreline velocity during both drawdown and runup stages, although the general trend is captured. A small amount of numerical instability can be seen near the shoreline (Fig. 5b), although it did not appear to affect the solution elsewhere.

Because extrapolation is used in the model, the convergence property of the model must be tested. We chose the error metrics to be the Root-Mean-Square (RMS) errors for the shoreline position and velocity as presented in Figure 5, and studied them as the grid resolution was varied. As indicated in ZHANG and BAPTISTA (2008), the Courant number is increased as the grid size is decreased, and by virtue of ELM, convergence is expected. This is indeed confirmed in Figure 6.

Volume and energy conservation is an important issue in tsunami applications (MYERS, 1998), which has caused serious problems in our application of ADCIRC. The total energy in the domain (at a particular time step) is:

$$E(t) = E_p + E_k, \tag{4}$$

Where the potential and kinetic energies are given by:

$$E_p = \frac{\rho g}{4} \int \eta^2 \, dA,$$
$$E_k = \frac{\rho g}{2} \int (|\mathbf{u}|^2 + w^2) \, dV. \tag{5}$$

Assuming that the outgoing wave travels at a speed of $\sqrt{gh}$, the energy flux across the right-hand boundary per unit length in the y direction and during each time step is then

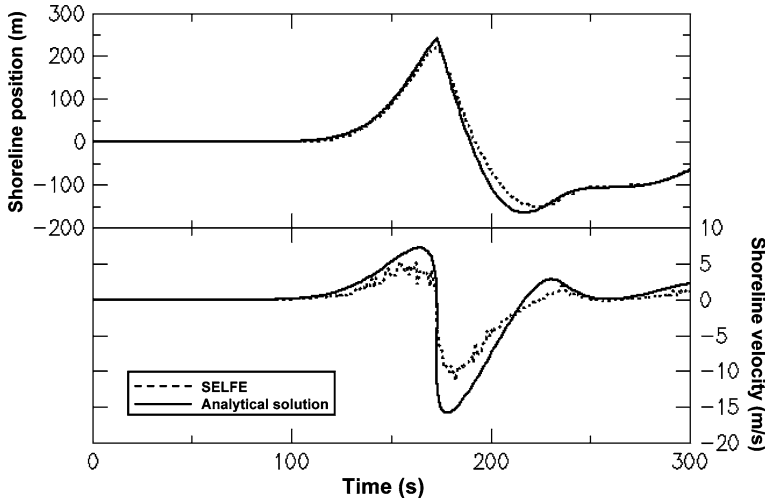

Figure 5
Comparison of time histories of shoreline position (top panel) and velocity at shoreline (bottom panel).

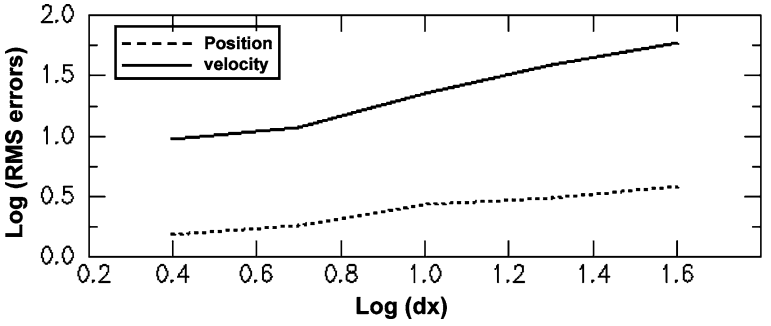

Figure 6
RMS errors in the predicted shoreline position and velocity as a function of grid size used, to show the convergence of the inundation algorithm. Log-log plot is used and the RMS error for the position is in m and that for the velocity is in m/s.

$$E_b = \frac{\rho \Delta t}{2}\left(g\eta^2 + h|\mathbf{u}|^2\right), \tag{6}$$

and the loss due to friction is:

$$E_f = \rho \Delta t \int C_D |\mathbf{u}|^3 dA, \tag{7}$$

where C_D is the friction coefficient. Since no bottom friction was used in this test, $E_f = 0$. An energy budget can then be constructed from Equations (4–7).

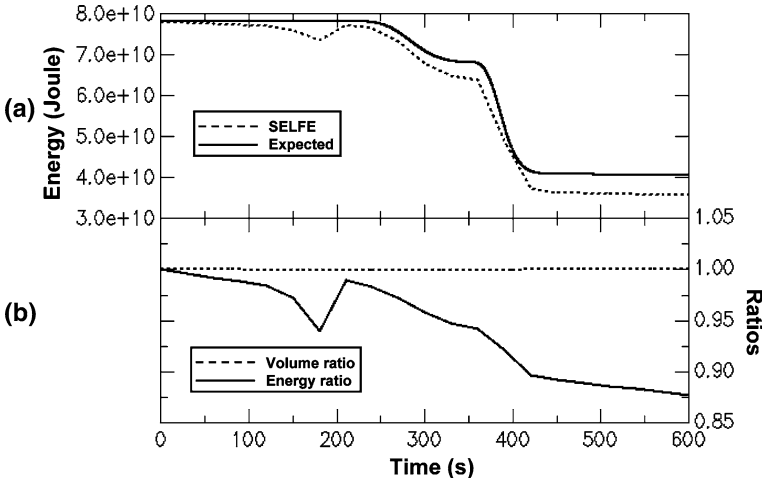

Figure 7
Energy and volume conservation in the plane beach test. (a) Time history of expected (analytical) and numerical total mechanical energies, accounting for the energy loss through the right open boundary. (b) Time history of volume ratio between expected and predicted volumes (both account for volume loss through the open boundary), and energy ratio between the energies shown in (a). The increase of the energy ratio around $t = 200$ s coincides with the inundation stage where extrapolation is used.

Starting from the potential energy in the initial *N*-wave, the time history of "expected" total energy can be calculated from the budget presented above. This is then compared with the actual amount of total energy in the model results in Figure 7. In addition, Figure 7b also shows the errors in volume conservation (a volume budget can be constructed by taking into account the water that leaves the domain during each time step). The volume conservation errors remain very small (<0.01%) throughout the entire simulation, which is in sharp contrast to the early ADCIRC results (unpublished). The actual energy is always smaller than the "expected" value, indicating a net loss. The temporary increase in energy during the runup stage (from $t = 180$ to 210 sec) is most likely due to the extrapolation used, which has added energy back to the system. The total energy loss at the end of 10 min is about 12.5%, which is a considerably better result than those from the ADCIRC runs (unpublished).

4.2. Wave Runup on a Complex 3-D Beach

The 1993 Hokkaido-Nansei-Oki tsunami serves as one of the best benchmark tests for inundation models because of the detailed bathymetric surveys before and after the event, and excellent field measurements. The earthquake occurred just west of Okushiri Island, and caused extensive damage along the Hokkaido coastline, however, the largest runup (up to 32 m) was observed at a narrow valley (Tsuji) within a small cove near Monai on the west coast of Okushiri Island (Shimamato *et al.*, 1995).

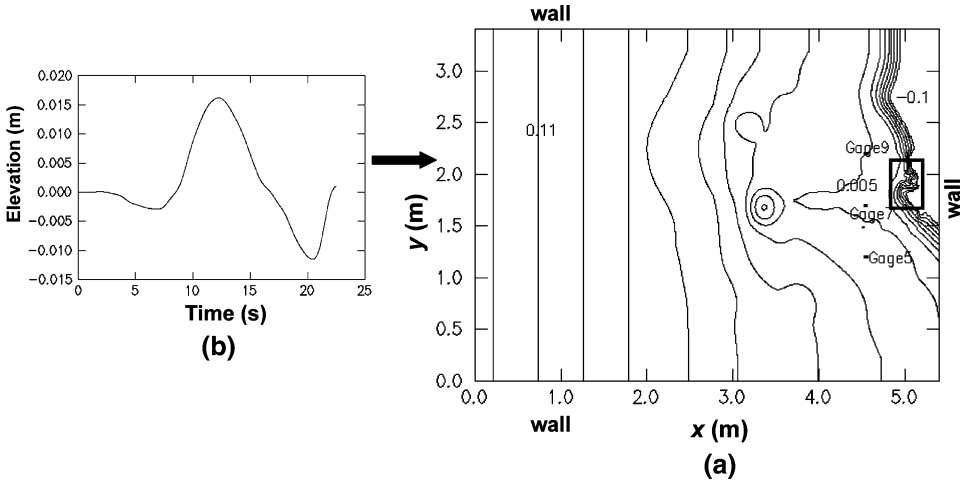

Figure 8
(a) Top view of the wave tank used in the laboratory test for the 1993 Okushiri tsunami. The increment between isolines is 0.015 m. The box indicates the approximate location of Tsuji valley where the largest runup was observed. Also shown are the locations of the three gages (5, 7, and 9) that measure the elevations. (b) The incoming *N*-wave profile.

In this section, we concentrate on the 1:400 scale laboratory experiment for this event, performed at Central Research Institute for Electric Power Industry (CRIEPI) in Abiko, Japan. The main theme of the experiment was to reproduce the largest runup around Monai, using a large-scale tank of 205 m long, 6 m deep, and 3.4 m wide (Fig. 8).

Figure 8 shows the set-up of the laboratory experiment and bathymetry and topography in the tank. It can be seen that the coastline is very complex especially near the Tsuji valley. The sidewalls at $y = 0$, and 3.5 m and $x = 5.49$ m are reflective. The incident *N*-wave from offshore, at the water depth $h = 13.5$ cm comes in from the left-hand side ($x = 0$). Therefore this is a boundary-value problem instead of an initial-value problem as in Section 4.1. The temporal variation of water surface elevation at three gages (Fig. 8) as well as animations of shoreline positions captured by three cameras are given on the IWLRM website. The maximum runups along the coast calculated from the MOST model (Titov and Synolakis, 1998) were also given in Chawla *et al*. (2007). Therefore we will compare SELFE results with the laboratory measurements at the three gages as well as the results presented in Chawla *et al*. (2007).

The model grid resolution is $\Delta x = \Delta y = 1.4$ cm (with each rectangle split into two triangles), roughly the same as the internal fine grid used in Chawla *et al*. (2007); again, we did not use a more efficient variable resolution unstructured grid for simplicity. As a result, the horizontal grid has 95892 nodes and 190512 elements. A time step of $\Delta t = 0.01$ sec, as in Chawla *et al*. (2007), was used. Similar to Section 4.1, the implicitness factor was set to be 1, bottom friction and viscosities were all neglected, and

two vertical layers were used in the vertical direction. The total duration of the run was 22.5 sec, which took 3.75 hours CPU time on the same platform as in Section 4.1.

The comparison of elevations at the three gages between SELFE and lab measurements is depicted in Figure 9; similar comparison can be found in Figure 4 of CHAWLA *et al*. (2007). The results for the first 10 sec are discarded because the model is still being ramped up. The overall agreement is satisfactory; the calculated maximum elevations at the three gages are within 4.6%, 5.1%, 4.6% of measure values, and lag the measured arrival times by 0.2, <0.001, and 0.1 sec, respectively; note the excellent match of arrival time at Gage 7. The results are also comparable to those in CHAWLA *et al*. (2007); the main difference occurs at Gage 9. While the simulated elevation at this gage in CHAWLA *et al*. (2007) was such that the position of the tide gage was dry from $t = 13.5$ to 15 sec, this gage is always submerged under water in our results, although the total water depths are very thin (<0.1 mm) during this period (Fig. 9b). The measured elevation at this gage is larger than those in either model (Fig. 9a).

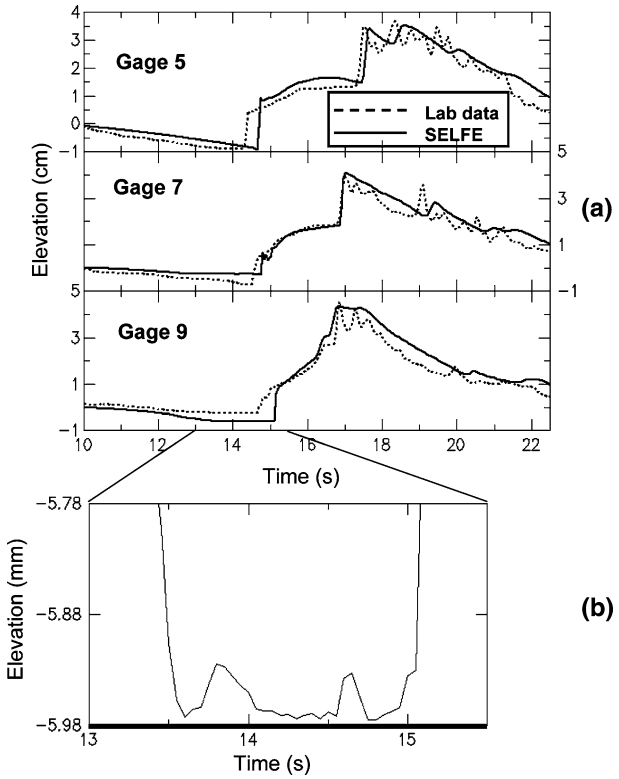

Figure 9

(a) Comparison of surface elevations at the gages shown in Figure 8. (b) Zoom-in of SELFE results at gage 9, where the depth is 5.98 mm (the bottom is indicated as the thick black line), from t = 13 to 15.5 s. Note that the total depth is positive despite being very small (<0.1 mm) between $t = 13.5$ s and 15 s.

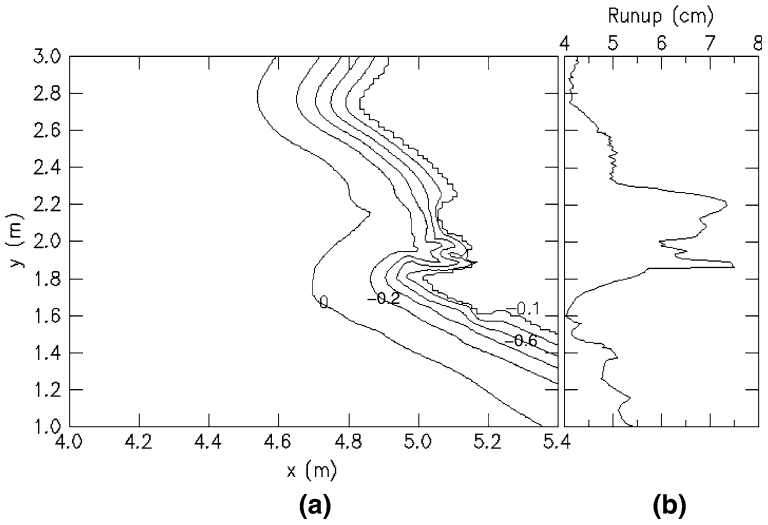

Figure 10
Maximum runup along the coastline. (a) Isobaths in the tank in the increment of 0.2 m; (b) maximum runup along the *y*-axis.

The calculated maximum wave runup around the Tsuji valley is shown in Figure 10, and can be compared to Figure 5 of CHAWLA *et al*. (2007). Both models predicted a large runup inside the cove, although the maxima there are different (10 cm for MOST vs. 7.5 cm for SELFE). If a linear scaling is assumed, the projected maximum runups in the cove for the real event are 40 m for MOST and 30 m for SELFE, with the field estimate being about 32 m. It should be emphasized that this simple scaling may not be appropriate as the experiment cannot faithfully reproduce all nonlinear processes that have occurred during the real event. Another peak in the runups north of the cove also appeared in both models, although at slightly different locations. Without actual measurements in this region, it is difficult to compare the two models there.

5. *Concluding Remarks*

A new tsunami model is proposed, and its ability to address stringent inundation benchmarks demonstrated. SELFE is based on the solution of the NSW equations with a semi-implicit finite-element method on unstructured grids, with Eulerian-Lagrangian treatment of advective terms in the momentum equation. A simple and yet effective inundation algorithm is incorporated in the model. Compared to a reference unstructured-grid tsunami model (ADCIRC), SELFE is computationally efficient, robust, accurate, and has improved volume and energy conservation properties. A parallel (MPI-based) version of the model, which has become available recently, will add to its attractiveness as a computationally efficient tool.

SELFE is in this paper benchmarked against two test problems: An initial-value problem with an analytical solution, and a laboratory experiment inspired by the 1993 Hokkaido-Nansei-Oki tsunami. Satisfactory results are obtained in both cases. We have also applied the SELFE to the 1993 Hokkaido-Nansei-Oki tsunami, with equally satisfactory results, which we will report in Part II. Applications of SELFE to the 1964 Alaska tsunami and to Cascadia Subduction Zone tsunamis are in progress; each application involves both an element of field validation and a re-assessment of the tsunami hazard for Oregon communities.

SELFE is a multi-purpose open source code, available at http://www.ccalmr.ogi.edu/CORIE/modeling/selfe/. Other applications of SELFE include studies of 3-D circulation in estuaries and plumes, reported elsewhere (ZHANG and BAPTISTA, 2008). The ability of SELFE to address fully 3-D problems effectively opens the opportunity for studies of sediment transport during tsunami events; a perspective that has strong potential value for Cascadia Subduction Zone tsunamis, whose strongest field evidence of inundation resides on sedimentary deposits.

Acknowledgements

The authors thank Dr. George Priest for his steadfast support, constant encouragement and guidance over the years. The Oregon Department of Geology and Mineral Industries and National Science Foundation (ACI-0121475; OCE-0424602) provided financial support for this research. Any statements, opinions, findings, conclusions, or recommendations expressed in this material are those of the authors and do not necessarily reflect the views or policies of the federal sponsors, and no official endorsement should be inferred.

REFERENCES

BAPTISTA, A.M. (1987), *Solution of Advection-dominated Transport by Eulerian-Lagrangian Methods Using the Backwards Methods of Characteristics*, Ph.D. Thesis, Massachusetts Institute of Technology (260 pp), Civil Engineering. Cambridge, Massachusetts.

BAPTISTA, A.M. (2006), *CORIE: The first decade of a coastal margin collaborative observatory*, Oceans'06 MTS/IEEE, Boston, MA.

BAPTISTA, A.M., PRIEST, G.R., and MURTY, T.S. (1993), *Field Survey of the 1992 Nicaragua Tsunami*, Marine Geodesy *16*(2), 169–203.

BAPTISTA, A.M., ZHANG, Y.L., CHAWLA, A., ZULAUF, M.A., SEATON, C., MYERS, E.P., KINDLE, J., WILKIN, M., BURLA, M., and TURNER, P.J. (2005), *A cross-scale model for 3D baroclinic circulation in estuary-plume-shelf systems: II. Application to the Columbia River*, Continental Shelf Res. *25*, 935–972.

BURWELL, D., TOLKOVA, E., and CHAWLA, A. (2007), *Diffusion and dispersion characterization of a numerical tsunami model*, Ocean Modelling *19*, 10–30.

CARRIER, G. F., WU, T. T., and YEH, H. (2003), *Tsunami run-up and run-down on a plane beach*, J. Fluid Mech. *475*, 79–99.

CASULLI, V. and WALTERS, R. A. (2000), *An unstructured grid, three-dimensional model based on the shallow water equations*, Int. J. Num. Meth. Fluids *32*, 331–348.

CHAWLA, A., BORRERO, J., and TITOV, V., *Evaluating wave propagation and inundation characterstics of the MOST tsunami model over a complex 3D beach*. In *Advanced Numerical Models for Simulationg Tsunami Waves and Runup* (eds. P. L.-F. Liu, H. Yeh, and C.E. Synolakis), vol. 10, *Advances in Coastal and Ocean Engineering* (World Scientific, 2008).

CHEN, C., H. LIU, H., and BEARDSLEY, R.C. (2003), *An Unstructured Grid, Finite-Volume, Three-Dimensional, Primitive Equations Ocean Model: Application to Coastal Ocean and Estuaries*, J. Atmos. Oceanic Tech. *20*, 159–186.

DIAS, F. and DUTYKH, D., *Dynamics of Tsunami Waves*, (Springer, Netherlands 2007).

DUTYKH, D., DIAS, F., and KERVELLA, Y. (2006), *Linear theory of wave generation by a moving bottom*, C. R. Acad. Sci. Paris, Ser. I, *343*, 499–504.

GEORGE, D. L. and LEVEQUE, R. J. (2006), *Finite volume methods and adaptive refinement for global tsunami propagation and local inundation*, Science of Tsunami Hazards *24*, 319–328.

GOLDFINGER, C., NELSON, C.H., and JOHNSON, J.E. (2003), *Holocene earthquake records from the Cascadia subduction zone and Northern San Andreas fault based on precise dating of offshore turbidites*, Ann. Rev. Earth Planet. Sci. *31*, 555–577.

HUBBARD, M.E. and DODD, N. (2002), *A 2-D numerical model of wave runup and overtopping*, Coastal Eng., *47*, 1–26.

KÂNOGLU, U. (2004), *Nonlinear evolution and runup–rundown of long waves over a sloping beach*, J. Fluid Mech. *513*, 363–372.

KÂNOGLU, U. and SYNOLAKIS, C.E. (2006), *Initial value problem solution of nonlinear shallow water-wave equations*, Phys. Rev. Lett. *97*(14), 148501.

LEVEQUE, R.J. and GEORGE, D.L., *High-resolution finite volume methods for the shallow water equations with bathymetry and dry states*. In *Advanced Numerical Models for Simulationg Tsunami Waves and Runup* (eds. P. L.-F. Liu, H. Yeh and C.E. Synolakis), vol. 10, *Advances in Coastal and Ocean Engineering* (World Scientific 2008).

LIU, L.-F., WU, T.R., RAICHLEN, F., SYNOLAKIS, C.E., and BORRERO, J.C. (2005), *Runup and rundown generated by three-dimensional sliding mass*, J. Fluid Mech. *536*, 107–144.

LIU, P. L.-F., YEH, H., and SYNOLAKIS, C.E. In *Advanced Numerical Models for Simulating Tsunami Waves and Runup* (eds. P. L.-F. Liu, H. Yeh, and C. E. Synolakis), vol. 10, *Advances in Coastal and Ocean Engineering* (World Scientific 2008).

LUETTICH, R.A., WESTERINK, J.J., and SCHEFFNER, N.W. (1991), *ADCIRC: An advanced three-dimensional circulation model for shelves, coasts and estuaries*, Coastal Engin. Res. Ct., U.S. Army Engs. Wtrways. Experiment Station, Vicksburg, MS.

LYNCH, D.R. and WERNER, F.E. (1991), *Three-dimensional hydrodynamics on finite elements. Part II: Non-linear time-stepping model*, J. Num. Meth. in Fluids *12*, 507–533.

LYNETT, P., WU, T.-R., and LIU, P.L.-F. (2002), *Modeling wave runup with depth-integrated equations*, Coastal Engin. *46*(2), 89–107.

MYERS, E.P., BAPTISTA, A. M., and PRIEST, G.R. (1999), *Finite element modeling of potential Cascadia subduction zone tsunamis*, Science of Tsunami Hazards *17*, 3–18.

MYERS, E.P. (1998), *Physical and numerical analysis of long wave modeling for tsunamis and tides*, Environmental Science and Engineering, Beaverton, Oregon, Graduate Institute of Science and Technology, 273 pp.

MYERS, E.P. and BAPTISTA, A.M. (1995), *Finite element modeling of the July 12, 1993 Hokkaido Nansei-Oki tsunami*, Pure Appl. Geophys. *144*(3/4), 769–801.

MYERS, E.P. and BAPTISTA, A.M. (1997), *Finite element solutions of the Hakkaido Nansei-Oki benchmark*. In *Long-Wave Runup Models* (eds. Yeh, H. *et al.*), pp. 272–280.

MYERS, E.P. and BAPTISTA, A.M. (2001), *Analysis of factors influencing simulations of the 1993 Hokkaido Nansei-Oki and 1964 Alaska tsunamis*, Natural Hazards *23*(1), 1–28.

PRIEST, G.R. (1995), *Explanation of mapping methods and use of the tsunami hazard maps of the Oregon coast*, Oregon Department of Geology and Mineral Industries, Open-File Report O–95-67, 95 pp.

PRIEST, G.R., ALLAN, J. C., MYERS, E.P., BAPTISTA, A.M., and KAMPHAUS, R. (2002), *Tsunami hazard map of the Coos Bay Area, Coos County, Oregon*, Oregon Department of Geology and Mineral Industries, Interpretive Map Series IMS-21.

PRIEST, G.R. and BAPTISTA, A.M. (2000), *Digital reissue of tsunami hazard maps of coastal quadrangles originally mandated by Senate Bill 379 (1995)*, Oregon Department of Geology and Mineral Industries, Open-File Report O-00-05, maps in.pdf and GIS formats and text files for Open File Reports O-95-38 and O-95-43 to O-95-67 [maps of the tsunami inundation zone (most probable Cascadia event) for the entire Oregon coast].

PRIEST, G.R., CHAWLA, A., and ALLAN, J.C. (2003), *Tsunami hazard map of the Alsea Bay (Waldport) area, Lincoln County, Oregon*, Oregon Department of Geology and Mineral Industries, Interpretive Map Series IMS-23.

PRIEST, G.R., MYERS, E., BAPTISTA, A.M., ERDAKOS, G., and KAMPHAUS, R. (1999a), *Tsunami hazard map of the Astoria area, Clatsop County, Oregon*, Oregon Department of Geology and Mineral Industries, Interpretive Map Series map IMS-11, scale 1:24,000.

PRIEST, G.R., MYERS, E.P., BAPTISTA, A.M., and KAMPHAUS, R. (1999b), *Tsunami hazard map of the Warrenton area, Clatsop County, Oregon*, Oregon Department of Geology and Mineral Industries, Interpretive Map Series IMS-12, scale 1:24,000.

PRIEST, G.R., MYERS, E.P., BAPTISTA, A.M., and KAMPHAUS, R. (2000), *Tsunami hazard map of the Gold Beach area, Curry County, Oregon*, Oregon Department of Geology and Mineral Industries, Interpretive Map Series IMS-13, scale 1:12,000.

PRIEST, G.R., MYERS, E.P., BAPTISTA, A.M., KAMPHAUS, R., PETERSON, C.D., and DARIENZO. M.E. (1997a), *Tsunami hazard map of the Yaquina Bay area, Lincoln County, Oregon*, Oregon Department of Geology and Mineral Industries: Interpretive Map Series IMS-2, scale 1:12,000.

PRIEST, G. R., MYERS, E.P., BAPTISTA, A.M., KAMPHAUS, R., PETERSON, C.D., and DARIENZO. M.E. (1998), *Tsunami hazard map of the Seaside-Gearhart area, Clatsop County, Oregon*, Oregon Department of Geology and Mineral Industries: Interpretive Map Series IMS-3, scale 1:12,000.

PRIEST, G. R., MYERS, E.P., BAPTISTA, A.M., KAMPHAUS, R., PETERSON, C.D., and DARIENZO. M.E. (1997b), *Cascadia subduction zone tsunamis: hazard mapping at Yaquina Bay, Oregon*, Oregon Department of Geology and Mineral Industries: 144.

PRIEST, G.R., QI, M., BAPTISTA, A.M., KAMPHAUS, R., C.D., and DARIENZO, M.E. (1995), *Tsunami hazard map of the Siletz Bay area, Lincoln County, Oregon*, Oregon Department of Geology and Mineral Industries: GMS-99, scale 1:12,000.

SHIMAMATO, T., TSUTSUMI, A., KAWAMOTO, M., MIYAWAKI, M., and SATO, H. (1995), *Field survey report on tsunami disasters caused by the 1993 Southwest Hokkaido earthquake*, Pure Appl. Geophy. *144*(3/4), 665-692.

SYNOLAKIS, C.E. and BERNARD, E.N. (2006), *Tsunami science before and beyond Boxing Day 2004*, Phil. Trans. R. Soc. A *364*, 2231–2265.

SYNOLAKIS, C.E., BERNARD, E.N., TITOV, V.V., KANOGLU, U., and GONZALEZ, F. (2007), *Standard, criteria, and procedures for NOAA evaluation of tsunami numerical models*, NOAA Technical Memorandum, OAR PMEL–135.

TITOV, V.V. and SYNOLAKIS, C.E. (1995), *Modeling of breaking and non-breaking long-wave evolution and runup using VTCS-2*, J. Waterway, Ports, Coastal and Ocean Engin. *121*(6), 308–316.

TITOV, V.V. and SYNOLAKIS, C.E. (1998), *Numerical modeling of tidal wave runup*, J. Waterway, Ports, Coastal and Ocean Engin. *124*(4), 157–171.

TSUNAMI PILOT STUDY WORKING GROUP (2006), *Seaside, Oregon Tsunami Pilot Study-Modernization of FEMA flood hazard maps*, NOAA OAR Special Report, Contribution No 2975, NOAA/OAR/PMEL, Seattle, WA, 83 pp. +7 appendices.

VENTURATO, A.J., ARCAS, D., and KANOGLU, U. (2007), *Modeling tsunami inundation from a Cascadia Subduction Zone earthquake for Long Beach and Ocean Shores, Washington*, NOAA Technical Memorandum, OAR PMEL-137.

WALTERS, R.A. (2005), *A semi-implicit finite-element model for non-hydrostatic (dispersive) surface waves*, Internat. J. Num. Meth. in Fluids *49*, 721–737.

WANG, K. and HE, J. (1999), *Mechanics of low-stress forearcs: Nankai and Cascadia*, J. Geophys. Res. *104*, 15191–205.

WEI, Y., BERNARD, E.N., TANG, L., WEISS, R., TITOV, V.V., MOORE, C., SPILLANE, M. HOPKINS, M., and KÂNOGLU, U. (2008), *Real-time experimental forecast of the Peruvian tsunami of August 2007 for U.S. coastlines*, Geophys. Res. Lett. *35*, L04609.

Westerink, J.J., Feyen, J.C., Atkinson, J.H., Luettich, R.A., Dawson, C.N., Powell, M.P., Dunion, J.P., Roberts, H.J., Kubatko, E.J., and Pourtaheri, H. (2004), *A new generation hurricane storm surge model for southern Louisiana*, http://www.nd.edu/∼adcirc/pubs/westerinketal_bams_ref1935b.pdf.

Witter, R.C., Kelsey, H.M. and Hemphill-Haley, E. (2003), *Great Cascadia earthquakes and tsunamis of the past 6700 years, Coquille River estuary, sourthern coastal Oregon*, Geolog. Soc. Am. Bull. *115*, 1289–1306.

Yalciner, A.C., Alpar, B., Altinok, Y., Ozbay, I., and Imamura, F. (2002), *Tsunami in the Sea of Marmara: historical documents for the past, models for future*, Marine Geology *190*(1–2), 445–463.

Zhang, Y.-L. and Baptista, A. M. (2008), *SELFE: A semi-implicit Eulerian-Lagrangian finite-element model for cross-scale ocean circulation*, Ocean Modeling *21*(3–4), 71–96.

Zhang, Y.-L., Baptista, A.M., and Myers, E.P. (2004), *A cross-scale model for 3D baroclinic circulation in estuary-plume-shelf systems: I. Formulation and skill assessment*, Continental Shelf Res. *24*, 2187–2214.

(Received January 1, 2008, revised June 25, 2008)
Published Online First: December 19, 2008